International Journal of Heat and Fluid Flow 000 (2016) 1–10

Contents lists available at ScienceDirect

International Journal of Heat and Fluid Flow

journal homepage: www.elsevier.com/locate/ijhff

Heat transfer characteristics of R-134a in a converging-Diverging nozzle

G.W. Mann*, G.R. Madamadakala, S.J. Eckels

Institute for Environmental Research, 64 Seaton Hall, Manhattan, KS 66506, United States

ARTICLE INFO

Article history:
Received 15 September 2015
Revised 21 June 2016
Accepted 22 August 2016
Available online xxx

Keywords:
Two-phase flow
Critical flow
Heat transfer enhancement
Cavitation
Sonic flow
Converging-diverging nozzle

ABSTRACT

Heat transfer characteristics of cavitating flows in the diverging section of a converging-diverging nozzle, with R-134a as the working fluid were investigated for mass fluxes from 11.3–52.3 kg m^{-2} s^{-1} and heat fluxes from 52.6–693 kW m^{-2}. Eleven different nozzle configurations were examined with different divergence angles, throat diameters, inlet profiles, and lengths. Heat flux measurement assumptions were analyzed using numerical conduction simulations with ANSYS Fluent. Experimental results indicated two different heat transfer regimes at high Reynolds number—one high and one low—likely due to wall dryout. A temperature drop with a strong correlation to Reynolds number as well as inlet profile was recorded due to the cavitation-induced phase change. Additionally, data showed two-phase heat transfer coefficients from 3.7 to as high as 285kW m^{-2} K^{-1}. Chen's correlation compared well with the recorded heat transfer coefficients for low Reynolds numbers. Variation of heat transfer coefficients with different geometry parameters were given, and potential sonic effects were discussed. With such high heat transfer coefficients, cavitation enhanced heat transfer in converging-diverging nozzles could be of significant use in electronics cooling applications.

1. Introduction

Cavitating flows, even through simple geometries, have complex flow dynamics and mechanisms that are difficult to analyze. In order to set the context for a discussion of these flows, we present a one dimensional, frictionless liquid flowing through the converging-diverging nozzle of Fig. 1. Below the nozzle are a set of pressure vs. distance curves illustrating the behavior of the fluid at successively lower back-pressures. The fixed inlet pressure (P_0) of the fluid is set above its initial saturation pressure.

Initially, with a back-pressure slightly below the inlet pressure (1), pressure drops at the throat due to the increase of velocity enforced by the continuity equation, but there is not phase change. Post-throat, pressure increases as cross-sectional area diverges. At some lower back-pressure (2), the low pressure region at the throat reaches the saturation point. Typically, this does not cause nucleation, as some superheat of the liquid is required to enact bubble formation (Vieira and Simoes-Moreira, 2007).

Further reduction in the back-pressure causes the liquid to enter a metastable state. This is denoted on Fig. 1 as the *nucleation region*. It is theoretically possible for nucleation to occur anywhere in this zone, either before or after the throat. Once nucleation occurs, bubbles will grow in finite time towards equilibrium. Though in some cases, equilibrium can be reached immediately via an expansion wave where the fluid properties discontinuously change across the wave front (Oza and Sinnamon, 1983; Simoes-Moreira and Shepherd, 1999; Vieira and Simoes-Moreira, 2007). Depending on the size of the bubbles, degree of superheat, velocity, and length of the nozzle, the fluid may or may not reach equilibrium by the exit.

Due to the fact that the speed of sound in a two phase mixture is significantly lower than speed of sound in either a saturated liquid or a saturated vapor, when nucleation actually occurs, the flow may immediately become supersonic. In the case of only sub-sonic flow upon nucleation, further acceleration of the flow or decrease of the sonic velocity may occur leading to the sonic condition (4). Any further reduction in the back-pressure after the sonic condition is reached does not increase the flow rate through the nozzle, i.e. the nozzle is choked. Additionally, after the sonic condition is reached, the pressure may continue to decrease in the *diverging* section of the nozzle, and the flow accelerate. While for single phase fluid, the local Mach number must be unity at the throat of the nozzle (in the inviscid case), in a two-phase fluid, because of metastable conditions and bubble dynamics, this may not occur (e.g. Shin and Jones, 1993; Vieira and Simoes-Moreira, 2007).

* Corresponding author.
E-mail addresses: gmann@ksu.edu (G.W. Mann), ganeshreddy.647@gmail.com (G.R. Madamadakala), eckels@ksu.edu (S.J. Eckels).

http://dx.doi.org/10.1016/j.ijheatfluidflow.2016.08.012
0142-727X/

Please cite this article as: G.W. Mann et al., Heat transfer characteristics of R-134a in a converging-Diverging nozzle, International Journal of Heat and Fluid Flow (2016), http://dx.doi.org/10.1016/j.ijheatfluidflow.2016.08.012

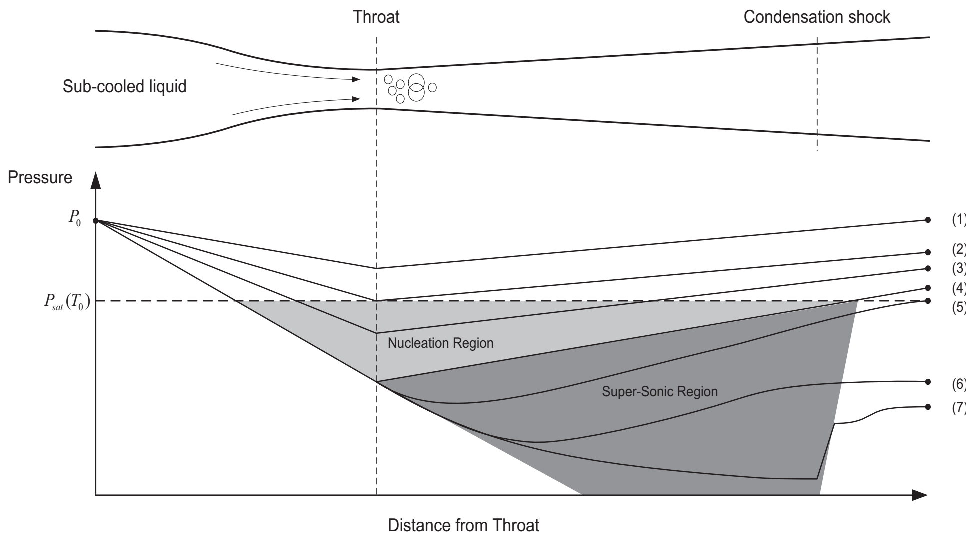

Fig. 1. Pressure lines for ideal flow through a converging-diverging nozzle.

The accelerating region of the fluid will continue along the diverging section. However, since the flow must meet the back-pressure condition, in the ideal case, a condensation shock, where the pressure discontinuously increases, will occur (7), as has been observed in Sandhu and Jameson (1979); Starkman et al. (1964). In non-ideal flow where viscous effects and acoustic dissipation can increase the pressure of the flow, the flow may not form a distinct condensation shock, but through a series of mini-shocks will transition slowly back to the back-pressure condition (6).

Various models have been proposed to predict the characteristics of cavitating flows. The classical method is to solve the 1D conservation equations for a homogeneous mixture. Doing this with an appropriate barotropic equation allows for critical flow rates and choked pressure ratios to be determined (see Henry and Fauske, 1971; Tangren et al., 1949 and review by Hsu (1972)). Extensions of this approach accounting for slip (Vogrin, 1963) or transport equations for void fraction (Goncalves, 2014) have been proposed. More complicated models solve the Rayleigh-Plesset bubble equation dynamically to address non-equilibrium effects (De Giorgi et al., 2010; Delale et al., 2014; Ishii et al., 1993; Noordzij and Van Wijngaarden, 1974; Preston et al., 2002).

For fluids that are used at working conditions sufficiently close to the critical point, generation of vapor bubbles causes local temperature of the fluid to decrease significantly. This has primarily been studied because of the way local temperature decrease at the vapor/liquid interface changes fluid properties and slows the growth rate of bubbles (De Giorgi et al., 2010; Franc et al., 2004; Goncalves, 2014; Tani and Nagashima, 2003). Very little work has been done exploring the affect local temperature drop has on heat transfer between the fluid and the wall. It is hypothesized that the temperature depression of the fluid combined with vigorous phase change along the nozzle stimulates high heat transfer coefficients. Understanding the relationship between the thermodynamic state of the fluid, geometry of the nozzle, and amount of heat transfer is important in various applications of this phenomena. For example, enhancing heat transfer in two-phase electronics cooling applications is continually important as chip power density increases. Additionally, evidence suggests that for some materials, cavitation damage is proportional to material temperature (Park et al., 2012); thus, predicting erosion rates and seal failure in control valves or pressure relief valves during cavitation may be improved by a knowledge of heat transfer between the flow and solid surfaces.

Recent work in this area has been performed for two-phase flow in microchannels. Schneider et al. (2006) consider cavitating flow through an orifice in a microchannel and measure heat transfer coefficients for different cavitating numbers. They show a 67% improvement in heat transfer over the non-cavitating case with heat transfer coefficients as high as 50 kW m^{-2} K^{-1}. Cole et al. (2006) explore whether this phenomena might be useful in a thermal management system. Sole et al. (2012) study a similar application of cavitation to microchannel heat transfer enhancement for R-134a, showing heat transfer coefficients as high as 100 kW m^{-2} K^{-1} for mass fluxes in the range of 500–1000 kg m^{-2} s^{-1}. Yuan et al. (2014) also study this enhancement, documenting an increase in heat transfer with an increase of heat flux and a decrease in quality. All of these studies focused on microchannel orifices.

More classic flow boiling has been experimentally studied in a broad range of geometries, conditions, and fluids. Examples of recent experimental heat transfer work with R-134a are Romstedt and Werner (1986) with mass fluxes from 50 to 200 kg m^{-2} s^{-1} and measured heat transfer coefficients from 5000 to 30,000W m^{-2} K^{-1}; Kanizawa et al. (2014) with mass fluxes from 75 to 200 kg m^{-2} s^{-1} and measured heat transfer coefficients from 1500 to 4000W m^{-2} K^{-1}; and do Nascimento et al. (2013) with mass fluxes from 400 to 1500 kg m^{-2} s^{-1} and heat transfer coefficients as high as 36kW m^{-2} K^{-1}. Most work has been done with lower mass fluxes than considered in this paper. One paper experimentally studying critical heat flux did study cases with mass fluxes in this range—up to 38,000 kg m^{-2} s^{-1} (Kaya et al., 2013). Only critical heat flux was reported; no heat transfer coefficients were given.

In this paper, heat transfer characteristics of cavitating two-phase flow through a converging-diverging nozzle are studied. A thermo-sensitive fluid—R-134a—is used. How different geometries and flow conditions affect temperature drop and local heat transfer coefficients is described. The remainder of the paper is organized as follows: Section 2 gives a description of the experimental setup, test conditions, data reduction, and uncertainty analysis, and in Section 3, results are presented and discussed.

2. Experimental description

2.1. Test section geometry

The nozzles used in this study were composed of multiple, cylindrical elements—or pucks—fastened together and sealed with O-rings (see Fig. 2a). This approach was prompted by